NORTHERN BORDER UNIVERSITY

Adsorption of Cr(VI) onto low-cost activated carbon: isotherm, kinetic and thermodynamic studies

Mohamed Ahmed Mahmoud
Department of Chemical Engineering, College of Engineering, Jazan University,
Jazan 45142, Saudi Arabia.

Abstract: The ability of commercial low-cost activated carbon (LC-AC) to adsorb and remove Cr Cr(VI) from the watery system was examined. The batch adsorption procedure investigated various limits for example pH, initial concentration, sorbent dosage, and interaction period. LC-AC was characterized using scanning electron microscopy (SEM). At pH 3.5 and 40 minutes, 6.22 mg/g was the highest adsorption capacity ever recorded. According to kinetic and equilibrium investigations, this process fits a second-order pseudo-model and a Langmuir isotherm. The Van't Hoff equation was utilized to evaluate the temperature-related variables, and the outcomes revealed that the procedure was exothermic. The enthalpy and average adsorption energy (E) values demonstrated that the adhesion action was physical in origin.

Keywords: Adsorption; Kinetic; Thermodynamic; activated carbon.

(*) **Corresponding Author**:

Mohamed Ahmed Mahmoud, Department of Chemical Engineering, College of Engineering, Jazan University, Saudi Arabia.

Jazan: 11592

E-mail: Momahmoud@jazanu.edu.sa

امتزاز الكروم السداسي على الكربون المنشط منخفض التكلفة: دراسات منحنيات الامتزاز والحركية والديناميكية الحرارية

د. محمد احمد محمود

قسم الهندسة الكيميائية، كلية الهندسة، جامعة جازان، جازان 45142، المملكة العربية السعودية.

مستخلص البحث: تـم فحـص قـدرة الكربـون المنشـط التجـاري منخفـض التكلفـة علـى امتصـاص وإزالـة الكـروم السداسـي مـن النظـام المائـي. عوامـل الامتـزاز الدفعـي المختلفـة مثـل الرقـم الهيدروجينـي، التركيـز الاولـى، وجرعـة المـادة الماصـة، وزمـن التفاعـل تـم التحقـق منهـا. تـم توصيـف الكربـون المنشـط باسـتخدام المجهـر الإلكترونـي الماسـح. عنـد درجـة حموضـة 3.5 و40 دقيقـة، كانـت 6.22 مجم/جـم أعلـى قـدرة امتصـاص تـم تسـجيلها علـى الإطـلاق. وفقـا لدارسـات الحركيـة والاتـزان، فـإن هـذه العمليـة تتناسـب مـع نمـوذج درجـة الحركيـة الرتبـة الثانيـة الزائفـة، ونمـوذج ايزوثيـرم لانجميـر. تـم اسـتخدام معادلـة فانـت هـوف لتقييـم المتغيـرات المرتبطـة بدرجـات الحـرارة، وأظهـرت النتائـج أن عمليـة الامتـزاز طـاردة للحـرارة. أظهـرت قيـم المحتـوى الحـراري ومتوسـط طاقـة الامتـزاز أن عمليـة الامتـزاز فيزيائيـة

كلمات مفتاحية: الامتزاز؛ الحركية؛ الديناميكا الحرارية؛ كربون منشط

(*) للمراسلة:
د. محمد احمد محمود، قسم الهندسة الكيميائية، كلية الهندسة، جامعة جازان، المملكة العربية السعودية.
جازان: 45142
E-mail: ribrahem@jazanu.edu.sa

1. Introduction

Chromium has negative environmental and health implications when used in excess. Before being released into the environment, effluent containing chromium must be treated to reduce contamination and related risks (Thirugnanasambandham and Shine, 2018). Numerous health issues, such as lung cancer, respiratory conditions, and skin irritation, may result from contact with high doses of Cr(VI) through drinking water besides inhalation (Mahmad et al., 2016; Abutaleb et al., 2023). Aquatic animals and ecosystems can be harmed by chromium pollution in water bodies, and sediment can become contaminated. Additionally, it may have an impact on crops and lower agricultural output (Genawi et al., 2020; Yan et al., 2023). Chromium can be eliminated from wastewater using a variety of techniques, including:

- Chemical precipitation (Nwabanne et al., 2018; Min et al., 2023): Chromium precipitates out of solution as an insoluble compound when chemicals like lime or ferrous sulphate are added to the wastewater. This insoluble product can then be removed by settling or filtration (Aoudj et al., 2017).

- Ion exchange (Elabbas et al., 2016): Chromium ions in wastewater can be selectively adsorbed and eliminated using ion exchange resins. The resin can be recycled after becoming fully saturated with chromium.

- Adsorption (Sadeghi et al., 2017; Abutaleb et al., 2021; Patil et al., 2023; Ayman et al., 2022): Through surface interactions, adsorbents like activated carbon or other unique adsorbents can remove chromium ions from wastewater.

- Membrane filtration (Singh et al., 2018): techniques like reverse osmosis and ultrafiltration enable water to flow

- Biological treatment (Ziati et al., 2018; Mubarak et al., 2024): Some microbes, including bacteria and fungi, have the ability to fix or decrease Cr(VI) to the less hazardous Cr(III). Wastewater treatment can make use of this bioreduction.

- Electrocoagulation (Elabbas et al., 2020): In this technique, wastewater is exposed to an electric current, creating a coagulant that makes it easier to remove chromium by flocculation and sedimentation. In this study, activated carbon which is widely available and reasonably priced was used to eradicate Cr(VI) ions from the watery system. This study looked into the abolition of Cr(VI) from liquid feed using common, inexpensive activated carbon. Cr(VI) uptake was investigated using contact time, starting metal ion concentration, pH, sorbent dosage, and temperature during experiments carried out

in a batch system. Investigations were made on the adsorption process's kinetics, isotherms, and thermodynamics.

2. Resources and approaches

2.1 Preparation of adsorbent material

Low-cost activated carbon (LC-AC) obtained as an agricultural byproduct (corn cob) was converted into low-cost adsorbent. At 450°C, the carbonization process took place, whereas the activation process was carried out in the presence of KOH.

2.2 Preparation of Cr (VI) stock solution

Dissolve the specified amount of $K_2Cr_2O_7$ in a watery system and dilute to the necessary attentiveness to produce a base solution containing 1000 mg/l Cr(VI). The chemicals were all AR grade and came from Sigma-Aldrich in Germany. 0.1N of NaOH and HCl were utilized to change the pH.

2.3 Batch experiment

The objective of the batch study is to examine the different conditions under which Cr(VI) adsorbs onto LC-AC. adding Cr(VI) preparations to Erlenmeyer flasks holding LC-AC is the process. Initial concentrations of 10–60 mg/L, pH ranges of 3–8, and variable durations of time at 30–60°C in a thermostatic shaking water bath are the parameters of the experiment. The water bath was shaken at 120 revolutions per minute using a thermostat. A five-minute centrifugation at 5000 rpm came after sample separation and agitation. The remaining Cr(VI) content was determined by a UV spectrophotometer (Perkin Elmer, A 800) at 370 nm. Adsorption capability (q) was defined as:

$$q = \frac{C_p - C_e}{M} \times V \tag{1}$$

Wherever

C_p = primary attentiveness of Cr(VI) (mg/L)

C_e = attentiveness of Cr(VI) at steadiness (mg/L)

V = bulk of Cr(VI) (L)

W = sorbent dosage of (LC-AC) (g)

According to the following equation, the removal percent (Re) is determined:

$$R_e \, (\%) = \frac{C_p - C_e}{C_0} \times 100 \tag{2}$$

Fig. 1 The series of experimentation sequence

3. Outcomes and discussion

3.1 LC-AC's characterization

SEM image of LC-AC prior to adsorption is shown in **Fig.2 (a)**. The surface appears to be irregularly shaped, rough, and porous. These features imply that the surface has a wide surface area and numerous fissures, which may enable effective adsorption between Cr(VI) ions and (LC-AC). Roughness and porosity give the Cr(VI) ions plenty of opportunities to interact with (LC-AC), possibly resulting in successful adsorption. The adsorption process may have caused certain alterations in the LC-AC based on the loss of porosity and roughness on the LC-AC surface **(Fig. 2(b))**. The Cr(VI) ions may have formed a connection with the surface, clogging the pores and smoothing out the imperfections. This change can be a sign that the target molecules were successfully adsorbed onto the LC-AC.

The N2-adsorption/desorption isotherms of LC-AC produced at 450 °C are shown in **Fig. 2(c)**. Based on IUPAC categorization, it indicates that the isotherm curves are most likely type I, indicating that the LC-AC is a microporous material with a surface area of 32.54 (m2/g) and a pore volume of 0.028 (cm3/g). There is a large range of pore diameters in materials, as indicated by the lack eyhof a distinct plateau.

.
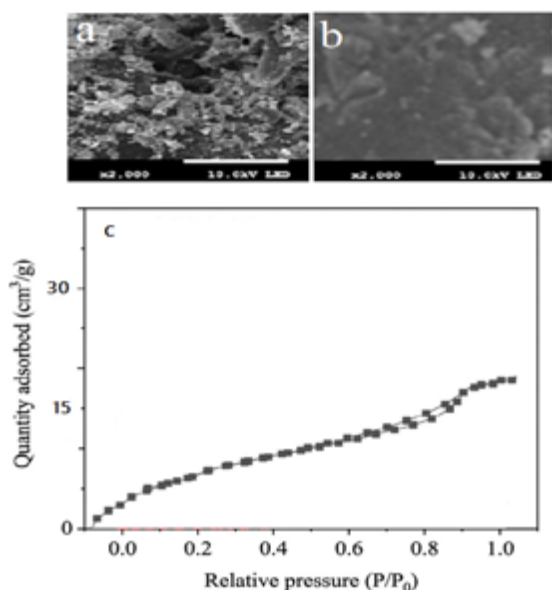
**Fig. 2 SEM image of Raw LC-AC (a) and Cr(VI) loaded LC-AC (b) N2 adsorption isotherm for activated carbon (c)**

3.2 Adsorption Investigations.

3.2.1 Result of pH:

The role of pH was examined by varying pH values from 3 to 8 at 30°C, 50 mg/l, 0.20 g/50 ml of adsorbent, 120 rpm of agitation, and 60 min **(Fig. 3)**.

The elimination efficiency of ions augmented at pH levels between 3 and 3.5. This indicates that as the pH rose within this range, more Cr(VI) ions were adsorbed onto the (LC-AC) material. At pH 3.5, the maximal capacity for Cr(VI) ions was attained. This shows that the (LC-AC) material had the greatest affinity for Cr(VI) ions at this particular pH. Lower pH levels (below 3.5) occasioned a reduction in the effectiveness of Cr(VI) ion removal. This might be because Cr(VI) ions and H+ ions are vying for the same adsorption sites on the (LC-AC) material. The amount of Cr(VI) ions that might be removed from the solution decreased as a result of this competition (Peng & Guo, 2020). The effectiveness of removing metal was reduced above a pH of 3.5. Hydrolysis, and chemical reaction in which molecules in water are broken down as a result of an increase in hydroxide ions (-OH) when the pH rises, is responsible for this decline in efficiency (Ali Maitlo et al., 2019).
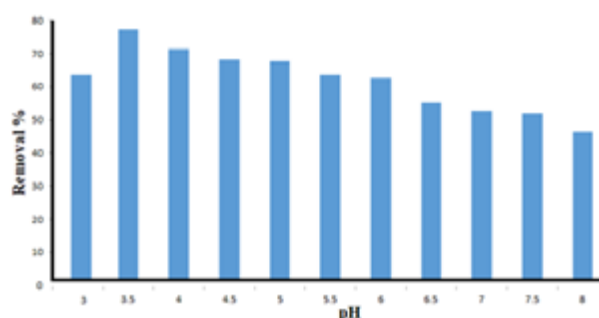
Fig. 3 Efficacy of pH on Cr (VI) ion binding to LC-AC

3.2.2 Effect of contact time:

The interaction period theatres a significant part in deciding how long it takes for the adsorbent (LC-AC) to absorb the greatest amount of the Cr(VI) adsorptive. The uptake procedure has more periods to take place the longer the contact time is. In your case, equilibrium is attained after 40 minutes under the indicated parameters of temperature (30°C), pH (3.5), and adsorbent dose (0.20g). As the contact period lengthens, Cr(VI) ion uptake also grows (Fig. 4). To be sure that the system genuinely reaches equilibrium, additional time may be allowed in some investigations, such as those that determine equilibrium adsorption isotherms. To better understand the uptake procedure, many kinetic replicas are being employed, e.g. pseudo-first-order, pseudo-second-order, Elovich, and intraparticle distribution.
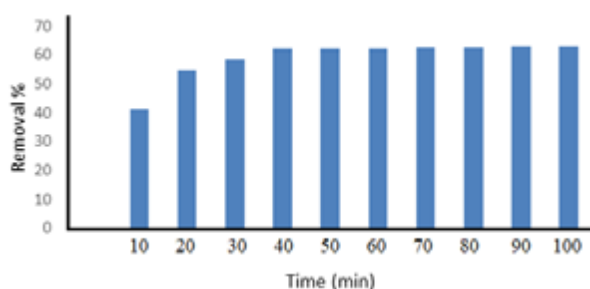
Fig. 4 Efficacy of interaction duration on the Cr (VI) elimination.

The pseudo-first-order kinetic model (Prasetyaningrum et al., 2018):

$$\log (q_e - q_t) = \log q_e - \frac{k_1}{2.303} t \tag{3}$$

The Pseudo-second-order model (Heffron et al., 2016):

$$\frac{t}{q_t} = \frac{1}{k_2 q_e^2} + \frac{1}{q_e} t \tag{4}$$

The Elovich model (Al-Qodah and Al-Shannag (2017):

$$q_t = \frac{1}{\beta} \ln(\alpha\beta) + \frac{1}{\beta} \ln(t) \tag{5}$$

The intraparticle diffusion model (Tejada-Tovar et al., 2020):

$$\log R_e = \log K_{id} + a \log(t) \tag{6}$$

Wherever qe & qt are the adhesion capabilities (mg/g) at stability and at time t, accordingly,, K1 and K2 are the factors of kinetic replicas. β & α are the Elovich coefficients. Kid is the Intraparticle constant. The rate-dependent compatibility of the experiment's results was examined by evaluating the correlation value (R2) (Prasetyaningrum et al., 2018).

$$R^2 = \frac{\sum_{i=1}^n (q_{e\ experimental} - q_{e\ theoritical})^2}{\sum_{i=1}^n (q_{e\ experimental} - q_{e\ theoritical})^2 + \sum_{i=1}^n (q_{e\ experimental} - q_{e\ theoritical})^2} \tag{7}$$

The larger R2 clearly demonstrated that the Cr(V1) adsorption kinetics closely resemble the pseudo-first-order model, as shown by Table 1 and Fig. 5. As a result, it became clear that physic-adsorption is crucial to the uptake of Cr(V1) by LC-AC (Mahmad et al., 2016).

Table 1. Adsorption kinetic model constants.

Models	Constant	Value
Pseudo-first-order	K1	0.090
	qe	1.666
	r2	0.996
Pseudo-second-order	qe	8.3961
	K2	0.0084
	r2	0.9566
Elovich	β	1.8231
	α	0.7898
	r2	0.9352
Intraparticle distribution	Kid	2.1592
	a	0.4246
	r2	0.8587
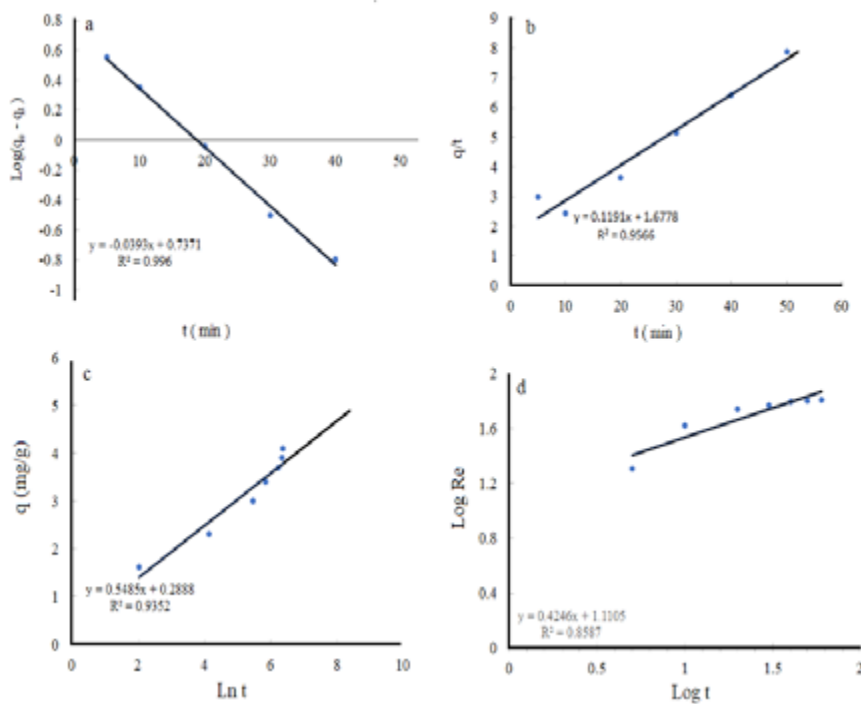
Fig. 5 Pseudo-first order (a) Pseudo-second order (b) Elovich (c) and Intraparticle diffusion (d) models.

21

3.2.3 Result of preliminary Cr(VI) concentrations:

The outcomes demonstrated that the adhesion capabilities rose from 3.32 to 6.22 mg/g as the starting Cr(VI) attentiveness augmented from 10 to 60 mg/L at 30°C, 0.20 g adsorbent dosage, 40 min, and pH 3.5. This indicates that while the starting concentration was higher, the adsorbent was able to trap more Cr(VI) ions. Additionally, the removal effectiveness decreased as the starting Cr(VI) content increased, indicating that the adsorbent was less efficient at eradicating Cr(VI) from the solution at higher preliminary concentrations and the open adsorption sites on the adsorbent became saturated (Khan et al., 2019). This shows that the accessible sites on the adsorbent are filled up as additional Cr(VI) ions are added to the solution, and eventually, no further adsorption can take place due to the adsorbent's limited capacity (He et al., 2020). To make the outcomes of experiments more accurate, the Freundlich isotherm and Langmuir replicas are used. Designing and improving adsorption methods for use in water treatment, pollution management, and other environmental applications requires the use of such data.

The Langmuir isotherm (Pavithra et al., 2020):

$$C_e/q_e = 1/Q_0b + C_e/Q_0 \qquad (8)$$

Where b (L/ mg) and Q0 (mg /g) are Langmuir coefficients.

The rudimentary qualities of the Langmuir faultless can be outlined using the distinction of dynamic RL (Liu et al., 2018).

$$R_L = \frac{1}{1 + b\,C_0} \qquad (9)$$

If 0 < RL < 1 implies that the binding mechanism is positive.

The Freundlich isotherm (Das and Nandi, 2020):

$$Log\,q_e = log\,(K_f) + 1/n\,log\,(C_e) \qquad (10)$$

In which KF and n are Freundlich parameters.

A better fit between the model and the experimental data is shown by higher R2 values (**Table 2**). There is a significant connection between the model and the data when the R^2 value is close to 1. The fact that the R2 value for the Langmuir isotherm is greater (0.983 > 0.921) shows that the Freundlich model does not adequately account for the investigational outcomes and that the Langmuir model does. From this, one can infer that the interaction of Cr(VI) onto LC-AC exists most likely the result of a monolayer adsorption process, as shown by the Langmuir isotherm (**Fig. 6**) (Chouhan et al., 2018).
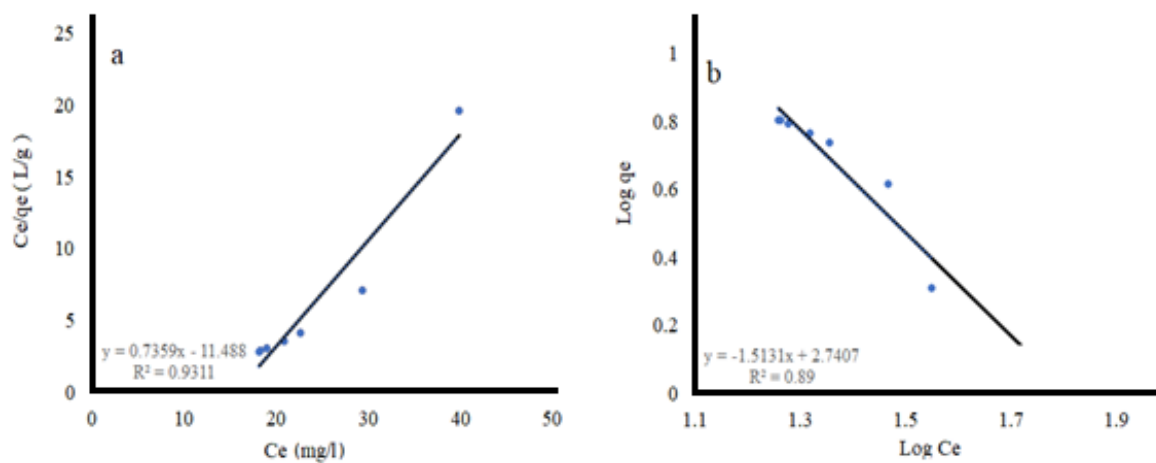

Fig. 6 (a) Langmuir (b) Freundlich isotherms of adsorption of process

Table 2. The adsorption system's Langmuir (a) and Freundlich (b) constants.

Langmuir				Freundlich		
b	Q0	RL	r2	Kf	n	r2
0.0640	1.358	0.6095	0.9311	6.6839	6.6608	0.890

3.2.4 Effect of adsorbent dose:

LC-AC was used in the experiment at different doses (0.01- 0.26g) for 40 minutes, pH 3.5 and 30°C. The elimination efficiency of Cr(VI) rose when the adsorbent dose augmented beginning 0.01g to 0.18g, as shown in Fig. 7. The attendance of extra energetic locations on the LC-AC may be due to the improvement in removal effectiveness with increasing adsorbent dosages. More adsorbent means more active sites for the Cr(VI) ions to bind to and be drawn out of the solution.

This is probably because bigger doses of the adsorbent have an increased surface area (Martín-Domínguez et al., 2018). However, subsequent increases in adsorbent dosage did not lead to a corresponding improvement in removal efficiency after a certain point (particularly when the adsorbent dose climbed beyond 0.18g). This shows that there is a limit to the benefits. At this point, the number of adsorbent particles may cause the adsorption sites to become congested, which could cause certain adsorption sites to overlap or become inaccessible (Emamjomeh et al., 2017).
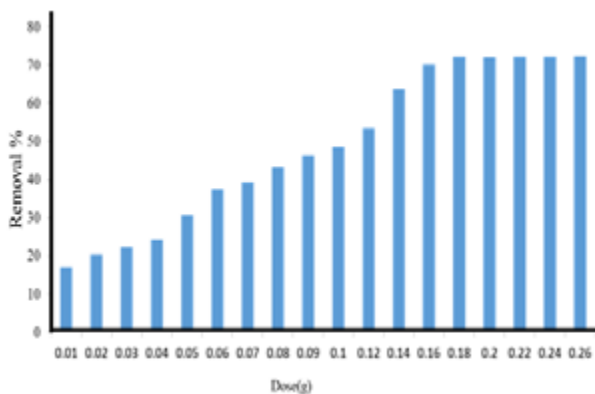

Fig. 7 The significance of LC-AC dosage on Cr(VI) removal.

3.3 Thermodynamic Studies

The temperature's effect on the Cr(VI) uptake was examined amid 30 and 60°C. As the temperature rose, It became apparent that eliminating Cr(VI) ions was less effective. The following equations (Babakhouya et al., 2019) were used to estimate the factors enthalpy ($\Delta H°$), entropy ($\Delta S°$), and Gibbs free energy ($\Delta G°$), using the diffusion coefficient (KD).

$$LnK_D = \frac{\Delta S°}{R} - \frac{\Delta H°}{RT} \tag{16}$$

$$K_D = \frac{q-}{Ce} \tag{17}$$

$$\Delta G° = \Delta H° - T\,\Delta S° \tag{18}$$

Table 3 shows that the -ve of $\Delta H°$ demonstrates that the adsorption procedure is exothermic. Also, the assessment of $\Delta H°$ can reveal information on the kind of adsorption (**Fig.8**) (Kim et al., 2020). The two primary categories are physical (physisorption) and chemical (chemisorption). In contrast to chemisorption, which typically involves greater heats of adsorption (80–200 kJ/mol), physical adsorption typically involves relatively lower heats of adsorption (2.1-20.9 kJ/mol) (Peng et al., 2019). Given that $\Delta H°$ has an absolute value of -5.278 kJ/mol (Table 4), The binding of Cr(VI) by LC-AC is most likely a physical sorption mechanism involving both types of elements. The minus sign of $\Delta G°$ demonstrates the potential and spontaneity of the act of adsorption, which means that the adsorption will take place naturally without the need for outside energy. During the solid/solution interface, a negative $\Delta S°$ denotes a reduction in unpredictability (Aboulhassan et al., 2018).

Table 3: Temperature-dependent thermodynamic variables.

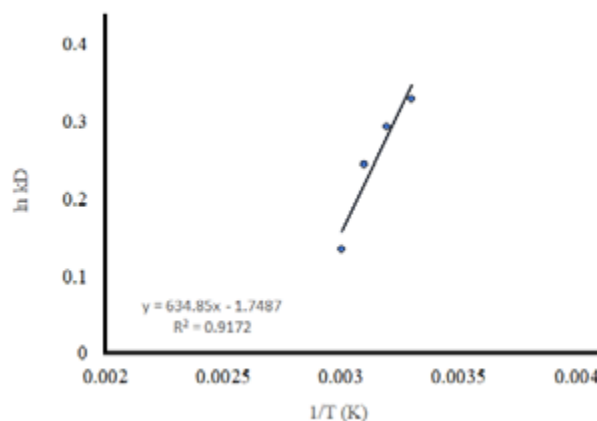| $\Delta H°$ (kJ/mol)	$\Delta S°$ (KJ/mol.K)	$\Delta G°$(kJ/mol)			
		30°C	40°C	50°C	60°C
-5.278	-0.0145	-0.8845	-0.7395	-0.5945	-0.4495

Fig. 8 ln KD vs 1/T(K) Van't Hoff conspiracy.

The energy change brought about by the transmission of a single mole of a sorbate species starting an infinitely diluted solution to the surface of a material is referred to as the mean free energy (E) of sorption. It offers an understanding of how the adsorbate and adsorbent surfaces interact using the following equations (Mamelkina et al., 2019).

$$E = RTLnK_D \qquad (16)$$

wherein R is the ideal gas standard (8.314 J/(mol. K)). The amount of mean free energy is able to reveal information about how strongly the adsorbate interacts with the adsorbent surface. Because temperature can affect the interactions between adsorbate and adsorbent, the mean free energy values varied with temperature. The binding mechanism is physical if E is less than 8 kJ/mol; otherwise, it is chemical. Where E exceeds 8 kJ/mol (Petrie et al., 2015). According to Table 4, as the temperature fluctuated between 30°C and 60°C, the mean free energy (E) changed from 2.799 to 5.559KJ/mol, respectively. The mean free energy values suggest that the physical-binding mechanism supported the results obtained by ΔH° value.

Table 4: Free Energy (E) at various temperatures.

Temperature °C	q (mg/g)	KD	E(KJ/mol)
30	6.22	0.329101	2.799
40	6.00	0.293399	3.19
50	5.45	0.243957	3.788
60	4.22	0.134181	5.559

4. Conclusions

This study's investigation of LC-AC revealed that it has good potential for purging water-based solutions of Cr(VI). At pH 3.5 and 40 minutes of contact time, the highest ability to adsorb (qe) ever recorded was 6.22 mg/g. The results of the kinetic and equilibrium analyses indicate that the procedure of binding matches the pseudo-second-order and the Langmuir isotherm. The uptake method is instantaneous and exothermic in nature. The LC-AC's binding of Cr(VI) is physical in nature, according to the estimated values of ΔH° and sorption energy (E).

5. Conflict of Interest

The authors have declared no conflict of interest

6. References

Aboulhassan, M. A., El Ouarghi, H., Ait Benichou, S., Ait Boughrous, A., & Khalil, F. (2018). Influence of experimental parameters in the treatment of tannery wastewater by electrocoagulation Separation Science and Technology (Philadelphia), 53(17), 2717-2726.

Abutaleb, A., Mohd, I., Nasser, Z., Afzal, H. K., Shahir, H., Mohammad, A. A., Omer, B., Mohammad, A. G., Nadeem, A. K., Hitesh, P., Sasan, Z. (2023). Fe3O4-multiwalled carbon nanotubes-bentonite as adsorbent for removal of methylene blue from aqueous solutions. Chemosphere 316,137824.

Abutaleb, A., Mubarak, A. E., Mohd, I., Kamal, K. T., Omer Y. B., Nasser, Z., Salah, E. F. H., Mohamed, H. (2021). Active adsorption performance of planetary ball milled Saudi Arabian bentonite clay for the removal of copper ions from aqueous solution Europhysics Letters 135 (3), 30005.

Al-Qodah, Z. & Al-Shannag, M. (2017). Heavy metal ions removal from wastewater using electrocoagulation processes: A comprehensive review Separation Science and Technology (Philadelphia), 52(17), 2649-2676.

Ali Maitlo, H., Kim, K. H., Yang Park, J., & Hwan Kim, J. (2019). Removal mechanism for chromium (VI) in groundwater with cost-effective iron-air fuel cell electrocoagulation Separation and Purification Technology, 213, 378-388.

Aoudj, S., Cheknane, B., Zemmouri, H., Zermane, F., Khelifa, A., Hecini, M., & Drouiche, N. (2017). Kinetics and adsorption isotherm for the removal of fluoride and chromium (VI) from wastewater by electrocoagulation Desalination and Water Treatment, 82, 262-270.

Ayman, Y., Ahmed, F.F. A., Nasser, Z., Mohamed, H., Mubarak, A. E., Haitham, M. H., Sahar, S., Ibrahim, M. M. (2022). The Enhanced Electrosorption Capacity of Activated Charcoal (AC) and WC@AC Composite for Water Desalination through Capacitive Deionization. Int. J. Electrochem. Sci., 17,22108.

Babakhouya, N., Abdouni, M., & Louhab, K. (2019). Electrochemical chromium(VI) recovery process by conducting composite, Olive Pomace/Pani Revue Roumaine de Chimie, 64(9), 747-753.

Chouhan, A., Thakur, L. S., Patidar, K., & Varma, A. K. (2018). A Review on Removal of Heavy Metals from Water / Wastewater by Electrocoagulation Process. International Research Journal of Engineering and Technology (IRJET), 5(12), 934-944.

Das, D. & Nandi, B. K. (2020). *Removal of Hexavalent Chromium from Wastewater by Electrocoagulation (EC): Parametric Evaluation, Kinetic Study and Operating Cost. Transactions of the Indian Institute of Metals, 73,* 2053-2060.

Elabbas, S., Ouazzani, N., Mandi, L., Berrekhis, F., Perdicakis, M., Pontvianne, S., Pons, M. N., Lapicque, F., & Leclerc, J. P. (2016). *Treatment of highly concentrated tannery wastewater using electrocoagulation: Influence of the quality of aluminium used for the electrode Journal of Hazardous Materials, 319,* 69-77.

Elabbas, S., Adjeroud, N., Mandi, L., Berrekhis, F., Pons, M. N., Leclerc, J. P., & Ouazzani, N. (2020). *Eggshell adsorption process coupled with electrocoagulation for improvement of chromium removal from tanning wastewater. International Journal of Environmental Analytical Chemistry. Advance online publication. https://doi.org/10.1 080/03067319.2020.1761963*

Emamjomeh, M. M., Jamali, H. A., & Moradnia, M. (2017). *Optimization of nitrate removal efficiency and energy consumption using a batch monopolar electrocoagulation: Prediction by RSM method. Journal of Environmental Engineering, 143(7),* 04017022.

Genawi, N. M., Ibrahim, M. H., El-Naas, M. H., & Alshaik, A. E. (2020). *Chromium removal from tannery wastewater by electrocoagulation: Optimization and sludge characterization. Water, 12(5),* 1374.

He, C., Gu, L., Xu, Z., He, H., Fu, G., Han, F., Huang, B., & Pan, X. (2020). *Cleaning chromium pollution in aquatic environments by bioremediation, photocatalytic remediation, electrochemical remediation and coupled remediation systems. Environmental Chemistry Letters, 18(3),* 561-576. *https://doi.org/10.1007/ s10311-019-00960-3*

Heffron, J., Marhefke, M., & Mayer, B. K. (2016). *Removal of trace metal contaminants from potable water by electrocoagulation. Scientific Reports, 6,* 28478.

Khan, S. U., Islam, D. T., Farooqi, I. H., Ayub, S., & Basheer, F. (2019). *Hexavalent chromium removal in an electrocoagulation column reactor: Process optimization using CCD, adsorption kinetics and pH modulated sludge formation. Process Safety and Environmental Protection, 122,* 118-130.

Kim, T., Kim, T. K., & Zoh, K. D. (2020). *Removal mechanism of heavy metal (Cu, Ni, Zn, and Cr) in the presence of cyanide during electrocoagulation using Fe and Al electrodes. Journal of Water Process Engineering, 33,* 101109.

Liu, T., He, F., An, C., Kang, X., Huang, Z., Li, W., & Zhang, Y. (2018). *Experimental study on the treatment of chromium containing wastewater by electric flocculation. IOP Conference Series: Earth and Environmental Science, 170(5).*

Mahmad, M. K. N., Rozainy, M. A. Z. M. R., Abustan, I., & Baharun, N. (2016). *Electrocoagulation Process by Using Aluminium and Stainless Steel Electrodes to Treat Total Chromium, Colour and Turbidity. Procedia Chemistry, 19,* 681-686.

Mamelkina, M. A., Vasilyev, F., Tuunila, R., Sillanpää, M., & Häkkinen, A. (2019). *Investigation of the parameters affecting the treatment of mining waters by electrocoagulation Journal of Water Process Engineering, 32,* 100929.

Martín-Domínguez, A., Rivera-Huerta, M. L., Pérez-Castrejón, S., Garrido-Hoyos, S. E., Villegas-Mendoza, I. E., Gelover-Santiago, S. L., Drogui, P., & Buelna, G. (2018). *Chromium removal from drinking water by redox-assisted coagulation: Chemical versus electrocoagulation Separation and Purification Technology, 200,* 266-272.

Min, K.J., An, H.J., Lee, A.H., Shin, H.-G., Park, K.Y. (2023). *Electrodialysis with a channeled stack for high strength cadmium removal from wastewater, Membr, Water Treat. 14,* 47–54.

Mubarak, A. E., Saleh, O. A., Mohamed, A. M., Isam Y. Q., Mohamed, H., Omer, Y. B., Gaber, A. E., Ahmed, F.F. A., Mohammad, S. A., Mustafa, S. E., Islam, G. A., Zeyad, M. A. (2024). *Enhancing photocatalytic performance of Co-TiO2 and Mo-TiO2-based catalysts through defect engineering and doping: A study on the degradation of organic pollutants under UV light Journal of Photochemistry & Photobiology, A: Chemistry 446,* 115164.

Naghdali, Z., Sahebi, S., Ghanbari, R., Mousazadeh, M., & Jamali, H. A. (2019). *Chromium removal and water recycling from electroplating wastewater through direct osmosis: Modeling and optimization by response surface methodology. Environmental Health Engineering and Management, 6(2),* 113-120.

Nwabanne, J. T., Igwegbe, C. A., & Okpo, S. O. (2018). *Removal of Copper, Nickel, and Chromium from Simulated Wastewater using Electrocoagulation Technique. 2018 International Conference Proceedings: Faculty of Engineering, Unizik, August,* 448-458.

Patil, Y., Attarde, S., Fegade, U., Bakather, O.Y., Ali, S.K. (2023). *Highly efficient removal of a toxic*

methylene blue dye by adsorption on CuAlMnO nanoparticles: adsorption kinetics, isotherm, and mechanism studies using statistical modelling. International Journal of Environmental Analytical Chemistry, 1-18.

Pavithra, K. G., Jaikumar, V., Kumar, P. S., & Sundarrajan, P. (2020). Cleaner strategies on the effective elimination of toxic chromium from wastewater using coupled electrochemical/ biological systems Environmental Progress and Sustainable Energy, 39(4), e13399.

Peng, H. & Guo, J. (2020). Removal of chromium from wastewater by membrane filtration, chemical precipitation, ion exchange, adsorption electrocoagulation, electrochemical reduction, electrodialysis, electrodeionization, photocatalysis and nanotechnology: a review. Environmental Chemistry Letters, 18, 2088-2068.

Peng, H., Leng, Y., & Guo, J. (2019). Electrochemical removal of chromium (VI) from wastewater. Applied Sciences, 9(6), 1156.

Petrie, B., Barden, R., & Kasprzyk-Hordern, B. (2015). A review on emerging contaminants in wastewaters and the environment: Current knowledge, understudied areas and recommendations for future monitoring. Water Research, 72, 3-27.

Prasetyaningrum, A., Jos, B., Dharmawan, Y., Prabowo, B. T., Fathurrazan, M., & Fyrouzabadi (2018). The influence of electrode type on electrocoagulation process for removal of chromium (VI) metal in plating industrial wastewater. Journal of Physics: Conference Series, 1025, 012126.

Sadeghi, S., Alavi Moghaddam, M. R., & Arami, M. (2017). Techno-economical evaluation of hexavalent chromium removal by electrocoagulation process with the aid of polyaluminum chloride as coagulant: Optimization through response surface methodology Environmental Engineering and Management Journal, 16(1), 93-104.

Singh, H., Sonal, S., & Mishra, B. K. (2018). Hexavalent chromium removal by monopolar electrodes based electrocoagulation system: Optimization through Box-Behnken design. Journal of Water Supply: Research and Technology - AQUA, 67(2), 147-161.

Tejada-Tovar, C., Villabona-Ortíz, A., & Ortega-Toro, R. (2020). Determination of Kinetic Parameters in the Biosorption of Chromium (VI) in Aqueous Solution Ingeniería y Ciencia, 16(31), 129-143.

Thirugnanasambandham, K. & Shine, K. (2018). Investigation on the Removal of Chromium from Wastewater using Electrocoagulation International Journal of Chemical Reactor Engineering, 16(5), 1-10.

Yan, B., Peng, J., Deng, F., Liu, L., Li, X., Shao, P., Zou, J., Zhang, S., Wang, J., Luo, X. (2023). Novel ZnFe2O4/Bi2S3 high-low junctions for boosting tetracycline degradation and Cr(VI) reduction, Chem. Eng. J. 452, 139353.

Ziati, M., Khemmari, F., Aitbara, A., & Hazourli, S. (2018). Reduction of Turbidity and Chromium Content of Tannery Wastewater by Electrocoagulation Process Water Environment Research, 90(7), 598-603.